Met O (APR) Turbulence and Diffusion Note No. 217b

The NAME 2 Dispersion Model: A Scientific Overview

by

D.B. Ryall & R.H. Maryon

March 1996

Met O (APR) (Atmospheric Processes Research)
Meteorological Office
London Road
Bracknell
Berkshire, RG12 2SZ

Note:

This paper has not been published. Permission to quote from it should be obtained from the Head, Atmospheric Processes Research, Met O(APR), Meteorological Office, London Road, Bracknell, Berkshire, RG12 2SZ.

The NAME 2 Dispersion Model: A Scientific Overview

D B Ryall & R H Maryon

March 1996

SUMMARY

The UK Meteorological Office's NAME model is used to simulate the medium and long range transport of a range of airborne pollutants. The model provides estimates of air concentrations and dosages, together with estimates of the deposition of pollutants to the ground by both wet and dry deposition processes. Wind fields and other meteorological data are obtained from global, regional and mesoscale versions of the UK Met Office's Numerical Weather Prediction Model (The Unified model). Applications include: emergency response (e.g. modelling accidental releases of radioactive material, such as in the Chernobyl incident); modelling the fate of sulphur emissions; and investigating the long-range transport of CFC's. For emergency response applications direct telecommunications links with the Department of Environment's Technical Coordination Centre allow rapid distribution of model products. As a WMO Regional Specialist Met Centre, the office also has international responsibilities for providing model forecasts in the event of an emergency.

The model has been recently been upgraded and improved in a number of areas. In particular, a nested mesoscale facility has been added, providing much improved resolution over the UK. To maximise the benefit of this enhanced resolution and extend the useful range of the model to shorter ranges, a new near-source diffusion scheme has been introduced. Other additions include improvements to the wet and dry deposition parametrizations, a scheme to represent plume rise for buoyant plumes, the introduction of a simple scheme to represent vertical mixing due to convection, a novel scheme allowing for small scale entrainments at the inversion, and improved output capabilities. This report describes the current model, NAME 2.1, its structure and capabilities, and the basis of the paramatrization of the underlying physical processes.

Contents

The NAME 2 Dispersion Model: A Scientific Overview

D B Ryall & R H Maryon

March 1996

1. INTRODUCTION

The NAME model is of a Lagrangian, Monte Carlo type in which emissions are modelled by releasing large numbers of 'particles' into the 'model atmosphere'. The particles are carried along passively by the ambient three-dimensional wind flow, with turbulent dispersion simulated by random walk techniques. Each particle represents a mass of released pollutant, which is reduced over time by both wet and dry deposition processes and radioactive decay. The model also has a 'radiological adjustment' package for modifying the plume spread and estimating source strengths from observational data.

This note gives a description of the model and its underlying physics. A general discussion of the principles, products and usage of the model can be found in the Users' Guide (Maryon & Ryall 1996), and details of the coding structure and submission procedures can be found in the program documentation (Ryall & Kitchen 1996). Further background information can be found in the previous model documentation (Maryon et al 1991, Kitchen 1993, Maryon 1993).

2. METEOROLOGICAL DATA

Underpinning the model is meteorological data from the global, regional and mesoscale versions of the UK Meteorological Office's numerical weather prediction (NWP) model, the Unified Model.

Grid	Area	Resolution (km)	F/C (hrs)	Levels used	Interval hrs
Global	Globe	90 km	144	12	6
Regional	N. Atlantic /Europe	50 km	36	12	3
Mesoscale	UK	17 km	24	24	1

Table 1.1 Unified model data used in NAME

The vertical coordinate of the unified model is the hybrid η (eta) coordinate which is related to pressure, p, by

$$\eta = \frac{p}{p_*} + A\left(1 - \frac{p_0}{p_*}\right)$$

where p_* is the surface pressure, p_0 is a reference pressure taken as 10^5 Pa, and A is a function of height. Near the surface A=0 so that the coordinate system follows the surface, then A varies with height until $A=\eta$ near the 'top' of the atmosphere, resulting in η following pressure levels. Whilst the global, regional and mesoscale unified models have 20, 20 and 30 η levels respectively; the NAME model currently uses 12,12 and 24 levels.

Figures 1-3 show the areas covered by the global, regional and mesoscale grids, together with their topography.

2.1 Availability

Forecast data for each of the model versions is held on-line, together with archives of recent data (approximately 14, 8 and 5 days for the global, regional and mesoscale archives respectively). Model simulations can span both analysis and forecast periods.

In addition a facility exists to reconstruct archives of analysis data. For the regional and global models meteorological data is kept for a period of two to three years, whilst mesoscale data is only available from mid 1995.

2.2 Nested Structure

The model has a 'nested' structure, whereby the meteorology used to advect and apply depositions to each particle is taken from the highest resolution data available for that location and time (to avoid boundary problems the outer 5 grid points on the mesoscale and regional grids are not used). Thus for example, a plume originating in the mesoscale area would be analysed at mesoscale resolution, while material passing out of the area is analysed using lower resolution regional data. Similarly particles may spread into a higher resolution grid from a lower resolution grid. A plume analysis may also pass to a coarser grid if, in forecast mode, longer range forecasts became available at the lower resolution. The model thus has a global capability, but with the benefit of being able to resolve plume development and resultant deposition to higher resolutions when and where higher resolution meteorological data are available.

2.3 High Resolution Data

In addition to the unified model precipitation products, a high resolution (6 km) map of *analysed* precipitation rates is available at hourly intervals. These are determined from the UK radar network (processed FRONTIERS images are used), the European radar network, satellite data, and mesoscale and regional NWP model output. Note that the high resolution data contains only total precipitation rates, and contains no information about precipitation type (i.e. convective or dynamic). The high resolution grid is also nested within the model, for use whenever and wherever it is requested

and data are available. Figure 4 shows the areal coverage of the high resolution rainfall data together with an example precipitation field.

2.4 Derived Fields

A number of derived fields are calculated from the unified model met fields; these include heights at model levels and boundary layer depths at model grid points.

2.4.1 Model Level Heights

To readily convert from η coordinates to height above ground (in metres), a three dimensional field of heights is generated. The thickness Δz of each model layer is determined from

$$\Delta z = \frac{R\overline{T}}{g}\log\left(\frac{p_1}{p_2}\right)$$

where p_1 and p_2 are the upper and lower pressure levels of the slab, R the gas constant for dry air and $\overline{T}$ the mean temperature of the slab. Pressures are determined from

$$p = Ap_0 + p_*(\eta - A)\,.$$

2.4.2 Boundary Layer Depths

The correct determination of boundary layer depth is crucial for modelling the dispersion of airborne pollutants and the resultant deposition to the ground (Maryon & Buckland 1994). For example, turbulent diffusion is significantly enhanced in the boundary layer, and only material in the boundary layer is subject to dry deposition. The advection of material will be adversely affected if the boundary layer depth is incorrectly diagnosed. In NAME, fields of boundary layer depths are calculated on the temperature grid from wind and temperature profiles, using either a Richardson number or parcel technique.

2.4.2.1 Richardson Number Technique

The presence of turbulent motion is inferred from the value of the gradient Richardson Number, R_i, which is calculated for a given model layer from

$$R_i = \frac{g\,\Delta\theta/\Delta z}{\overline{T}(\Delta u/\Delta z)^2}$$

where $\Delta\theta/\Delta z$ and $\Delta u/\Delta z$ are gradients of potential temperature and wind speed, g is the acceleration due to gravity and $\overline{T}$ is the mean temperature of the layer. This is calculated for each model 'slab' (bounded by model levels) until the Richardson number exceeds a critical value, R_{ic}, taken as 1.3. This high value is derived from earlier investigations with the operational NWP models, and is intended to offset the loss of detail in the model profiles due to discretization (indeed, comparisons of model

profiles with radiosondes would suggest an even larger R_{ic} is needed). The boundary layer top (in η) is then taken as the bottom of the slab for which R_{ic} is exceeded.

As the wind and temperature grids are staggered, the wind values must be bilinearly interpolated to temperature grid points before the boundary layer depths can be calculated.

2.4.2.2 Parcel Method

In the parcel method the dry adiabatic lapse rate (DALR) is followed from the surface (more strictly 1.5m) temperature, and the height at which it intersects the model environment curve (as defined by the model temperature profile) determined. Before following the DALR 1.2 °C is added to the 1.5m temperature unless the surface layer is stable, in which case 0.5 °C is added (this latter allowing for certain anomalies found in daytime ascents). A detailed rationale for the technique is contained in Maryon & Best (1992).

2.4.2.3 Implementation

The boundary layer depth is taken as the maximum of the Richardson Number and parcel method values. This generally results in the Richardson Number method being used in stable conditions and the parcel method in unstable conditions. A minimum boundary layer depth of about 80m (η = 0.99) is used, and a maximum boundary layer top of η = 0.55 (approx. 5000 m).

2.5 Output Grids

For convenience and easy comparison diagnostic fields such as air concentrations, dosages and depositions are generated on the unified model grids (the centre of each analysis cell being defined by the NWP 'temperature' grid points) and the high resolution rainfall grid. In addition fields can be output on (i) a latitude/longitude grid of user-defined size, origin and resolution---the latest diffusion schemes permit the definition and use of very high resolution near-source grids---and (ii) a 20km grid based on the national grid, covering the united kingdom. Air concentrations are determined for a number of vertical slabs, which are user-definable. By default nine vertical levels are used (the same levels are used for all output grids).

3. RELEASE

In the NAME model the pollutant is represented by large numbers of particles 'released' into the model atmosphere. Each particle can represent the mass or activity of a number of pollutant species. In what follows 'mass' represents either mass or radioactivity.

3.1 Source Definitions

A number of 'sources' can be defined, each source being defined by its location, start and end time of release, lower and upper vertical limits (in η units), and release rate

for each species. Thus complex release profiles as a function of time and height can be constructed by the use of several 'sources'. Similarly, several release locations can be represented. The location of a source can be defined in latitude/longitude, national grid or unified model grid coordinates.

Simple rectangular area sources can be represented by defining a length in the x and y directions (in the same coordinate system as the release point is defined). Each particle released from an area source is given an initial x,y coordinate randomly chosen from within the area. Simple line sources aligned north-south or east-west can be defined simply by adopting a zero length in the appropriate direction.

For sulphur modelling, point sources are used to represent major sources such as power stations, with other sources represented by area sources.

3.2 Implementation

Each timestep all sources are checked to determine whether a release is required for the current time. The vertical coordinate is chosen randomly between the upper and lower limits, and the time of release chosen randomly within the timestep. The number of particles released per source is $N=P\Delta t$, where P is the particle release rate, and Δt is the timestep. Alternatively, the number of particles released can be based on a user-defined particle mass, i.e. $N=R\Delta t/M$ where R is the mass release rate and M is the user-defined particle mass. A minimum particle mass can be defined such that no particle is released if its initial mass is below this mass, if a minimum particle mass is not defined then at least one particle is released from each 'live' source per timestep.

4. ADVECTION AND DISPERSION

4.1 Introduction

Particles are advected in three dimensions by model winds, with turbulent dispersion simulated by random walk techniques which take into account the ambient turbulent velocity structures. The random velocity components are functions of the vertical profiles of the vertical velocity variances and Lagrangian timescales, which are mostly derived from published empirical fits to observational data. Separate formulae are used for stable and unstable conditions. For unstable conditions both Gaussian and non-Gaussian (skewed) turbulence schemes are available.

Details of the broad integration strategy, loops, timestepping, etc, can be found in the model documentation (Ryall & Kitchen, 1996).

4.2 Meteorological Data

All meteorological data are linearly interpolated in space (either 2D or 3D depending on data type) to particle positions, and in time to the start of the current model step.

4.3 Random Walk Technique

The description of the random walk technique is summarised from Physick & Maryon (1995), although later revisions have been incorporated.

Particles are advected each timestep using

$$\mathbf{x}_{t+\Delta t} = \mathbf{x}_t + [\mathbf{u}(x_t) + \mathbf{u}'(x_t)]\Delta t \qquad (4.1)$$

where $\mathbf{x}(x,y,\eta)$ are the particle position vectors, $\mathbf{u}(x,y,\eta)$ and $\mathbf{u}'(x,y,\eta)$ the wind velocity and turbulent velocity vectors, and Δt is the timestep.

The subgrid velocities are obtained from a differential equation, first proposed by Langevin in 1908 as a model for Brownian motion. Although a general form of the Langevin equation exists which is valid for non-stationary, non-Gaussian (skewed) and inhomogeneous turbulence (Thomson, 1987), simpler forms of this equation can be applied when the turbulence is assumed to be Gaussian or homogeneous. By skewed it is meant that the probability that a sampled vertical velocity will be positive is not the same as that it will be negative; in Gaussian turbulence the probabilities are equal. An example of the former is convective turbulence, where downdraughts occupy a greater area than updraughts and are in general weaker. By inhomogeneous, we mean varying in the vertical (turbulence is assumed homogeneous in the horizontal). In the following sections we present the different forms of the Langevin equation used in the model according to the type of turbulence being parametrized.

4.3.1 Horizontal Motion

Assuming that the components of the turbulent motions are uncorrelated, the turbulent velocity component in the x direction is obtained from the differential equation

$$du' = a\,dt + b\,d\xi \qquad (4.2)$$

where the first term on the right hand side represents a 'memory' of previous motion and the second term an innovation. The coefficients a and b are defined by

$$a = -\frac{u'}{\tau_x}$$

$$b = \left(\frac{2\sigma_u^2}{\tau_x}\right)^{0.5}$$

where τ_x is the Lagrangian timescale for the x component of the turbulence and σ_u^2 the horizontal velocity variance. The $d\xi$ are increments of a random process; they are here taken as Gaussian with mean zero and variance dt. Thus the turbulent velocity component can be expressed as

$$u'_{t+\Delta t} = u'_t\left(1-\frac{\Delta t}{\tau_u}\right)+\left(\frac{2\sigma_u^2\Delta t}{\tau_u}\right)^{1/2} r_t \qquad (4.3)$$

where r_t is a random Gaussian variable of zero mean and unit variance. The expression for the v component is similar.

4.3.2 Vertical Motion

4.3.2.1 Gaussian Turbulence

Whilst this formulation is adequate for the u and v components, where changes in the horizontal are small, the situation in the vertical is more complex as σ_w is not constant with height, resulting in particles tending to collect at levels of small σ_w. To account for this we use:

$$w'_{t+\Delta t} = w'_t\left(1-\frac{\Delta t}{\tau_w}\right)+\left(\frac{2\sigma_w^2\Delta t}{\tau_w}\right)^{1/2} r_t + \frac{\Delta t}{\sigma_w}\frac{\partial \sigma_w}{\partial z}\left(\sigma_w^2 + w_t'^2\right) \qquad (4.4)$$

which is equivalent to the Wilson-Thomson (1983) model described in Physick & Maryon (1995). The final term on the right represents a 'drift' velocity', which prevents particles collecting in regions of low σ_w. When homogeneous turbulence profiles are used $\partial \sigma_w / \partial z = 0$, so the drift velocity term is zero.

4.3.2.2 Skewed Turbulence

Under one option the turbulence profile in the convectively unstable boundary layer can be assumed non-Gaussian (i.e. skewed). Once again, the general form of the Langevin Equation (4.2) is used, but the drift and diffusion coefficients a and b are specified differently. The corresponding equation to (4.2) is

$$dw' = adt + bd\xi \qquad (4.5)$$

where $b = (C_0\varepsilon)^{1/2}$, ε is the rate of dissipation of turbulent kinetic energy and C_o is a universal constant. Uncertainty surrounds the value of C_o, although 2.0 is usually used for unstable conditions. The Lagrangian timescale τ_w can be related to ε by the relation

$$\tau_w = \frac{2\sigma_w^2}{C_0\varepsilon} .$$

The coefficient a is a function of Σ_w and l, both measurable quantities, rather than τ_w which is only clearly defined when the turbulence is homogeneous and stationary. Note too that it is not necessary to incorporate the skewness Sk of the convective boundary layer in the diffusive (random) term, which remains Gaussian. Thus the finite-difference form of Equation 4.5 is

$$w'_{t+\Delta t} = w'_t + a\Delta t + \left(C_0\varepsilon\Delta t\right)^{1/2} r_t .$$

An expression for the function a is obtained by solving the following form of the Fokker-Planck equation (Thomson, 1987),

$$\frac{\partial (aP_E)}{\partial w} = -\frac{\partial P_E}{\partial t} - \frac{\partial (wP_E)}{\partial z} + \frac{1}{2} C_0 \varepsilon \frac{\partial^2 P_E}{\partial w^2} \qquad (4.7)$$

subject to the boundary condition $aP_E \rightarrow 0$ as $| w' | \rightarrow \infty$. P_E is the probability density function (PDF) made up of two Gaussian functions, one representing the updraughts (+) and the other representing the downdraughts (-) of the convective boundary layer, and written as

$$P_E = pN(m_+, \sigma_+) + (1-p)N(m_-, \sigma_-)$$

with

$$N(m, \sigma) = \frac{(2\pi)^{-0.5}}{\sigma} \exp\left(-\frac{(w' - m)^2}{2\sigma^2} \right).$$

Here p is the probability of a particle being in an updraught, m_+ is the mean velocity in an updraught and σ_+ is the velocity standard deviation in an updraught, and similarly m_-, σ_- for the downdraught terms. The first three moments of P_E are equated to the first three moments of the vertical velocity distribution ($0, \sigma_w^2$ and S_w^3 respectively, where $S_w^3 = Sk\,\sigma_w^3$) and the resulting equations are solved for the variables p, m_+ and m_-, by making the assumption $\Sigma = |m|$ for both updraughts and downdraughts (see for example Hudson and Thomson, 1994). The solutions are

$$p = 0.5\left(1 - \left(\frac{Sk^2}{8 + Sk^2} \right)^{0.5} \right) \qquad (4.8)$$

$$m_+^2 = \frac{0.5\sigma_w^2 (1-p)}{p} \qquad (4.9)$$

$$m_- = -\frac{m_+ p}{1-p} \qquad (4.10)$$

where $Sk = (S_w/\Sigma_w)^3$ is the degree of skewness of the turbulence.

By means of a little calculus, the solution of Equation 4.7 can be shown to be (see for example Luhar and Britter, 1989)

$$a = \frac{\phi_+ + \phi_-}{P_E} \qquad (4.11)$$

where

$$\phi_+ = -\frac{1}{2}C_0\varepsilon pN_+(w' - m_+)/\sigma_+^2 +$$

$$\sigma_+ N_+\left(\frac{\partial p\sigma_+}{\partial z} - \frac{pw'}{\sigma_+^2}\left(m_+\frac{\partial \sigma_+}{\partial z} - \sigma_+\frac{\partial m_+}{\partial z}\right) + \frac{pw'^2}{\sigma_+^2}\frac{\partial \sigma_+}{\partial z}\right)$$

$$-\frac{1}{2}\frac{\partial pm_+}{\partial z}\left(1 + erf\left(\frac{w - m_+}{\sqrt{2}\sigma_+}\right)\right)$$

with the expressions for ϕ_- of the same form, except with p replaced by $1-p$ and with subscript "+" replaced by "$-$". Note that due to the relation between m_+ and m_- the inner bracket in the second term is zero, and $(1 + erf)$ can be replaced simply with *erf*, when the + and $-$ terms are combined.

4.3.3 Computational Timestep

It is necessary to define a computational timestep such that the change in magnitude of σ_w should be small in comparison to σ_w itself, i.e.

$$w'\Delta t\left|\frac{d\sigma_w}{dz}\right| << \sigma_w,$$

so that

$$\Delta t << \frac{1}{|d\sigma_w/dz|}.$$

For practical purposes

$$\Delta t = \frac{e_1}{|d\sigma_w/dz|},$$

where e_1 is a small number such as 0.05 or 0.1. However, this may lead to large values near $d\sigma_w/dz = 0$, so it is replaced by

$$\Delta t = \frac{e_1 z_i}{|w'|}$$

if smaller, where z_i is the boundary layer depth (replaced by z if $z > z_i$).

In addition, the timestep must be short in comparison with the Lagrangian timescale, so that the additional restraint of

$$\Delta t \leq e_2\tau_w$$

is applied, where e_2 is another small number. In order to avoid too short a timestep, the Lagrangian timescales for all stabilities are subject to a minimum of 20 seconds, although in reality they may well be smaller near the surface.

4.3.4 Long Range Scheme

The random walk technique is computationally expensive, so a simpler scheme is used at longer ranges. A fixed timestep Δt_d is used (i.e the timestep of the main loop, typically 5,10 or 15 mins---see Ryall & Kitchen 1996), and the turbulent component is determined under the assumption $\Delta t = \tau$ so that the memory term is excluded (see expression 4.3). Values for σ and τ (horizontal and vertical) are determined from homogeneous profiles, and an effective velocity variance σ_{eff} determined appropriate to the timestep Δt_d, which preserves an appropriate diffusion coefficient K. That is,

$$K = \sigma^2\tau = \sigma^2\Delta t = \sigma_{eff}^2 \Delta t_d$$

then

$$\sigma_{eff} = \sqrt{\frac{\sigma^2\tau}{\Delta t_d}},$$

and from equation 4.3 ,

$$u' = \sqrt{2}\sigma_{eff} r_i .$$

Similarly for the other components. Advection is then by equation 4.1, producing, of course, the parabolic spread which results from this type of formulation (a Wiener process yielding standard diffusive spread).

4.4 Turbulence profiles

The remainder of the random walk formulation consists of the derivation of suitable values for the vertical profiles of σ and the Lagrangian timescale τ or turbulence dissipation rate ε. These will depend on the stability of the atmospheric boundary layer. As turbulent kinetic energy is not available from the Unified Model, the values must be determined either from empirical fits to observational data, or parametrized from information available from the Unified Model, e.g. by Richardson number formulae. The first option has been chosen for the NAME 2 parametrization. For the unstable boundary layer, we employ the turbulence profiles of Hibberd and Sawford (1994) and Hurley and Physick (1993), with a mechanical component or neutral limit from Brost et al (1982).

Both inhomogeneous profiles (σ & τ a function of height within the boundary layer) and homogeneous profiles (σ & τ constant within the boundary layer) are available. The inhomogeneous profiles are the most accurate whilst the use of homogeneous profiles offers the advantage of computational speed.

4.4.1 Determination of Stability

The stability of the boundary layer is determined from the Monin-Obhukov length:

$$L = -\frac{\rho c_p T_s u_*^3}{kgH}$$

where ρ is air density, c_p is the specific heat at constant pressure, k is von Karman's constant, T_s the surface temperature, H the sensible heat flux and u_* the friction velocity. Negative values of L indicate unstable boundary layers. The convective velocity scale w_* is determined from

$$w_* = u_* \left(\frac{k z_i}{|L|} \right).$$

4.4.2 Stable Conditions

4.4.2.1 Inhomogeneous profiles

At night the atmosphere becomes stably stratified due to radiative cooling from the surface beneath, and turbulence tends to be suppressed. Typically it takes the form of slow oscillations of wind direction with intermittent bursts of mechanically driven turbulence, depending on the wind strength. The profiles adopted for the present are (Hanna 1982)

$$\sigma_u = \sigma_v = 2.0 u_* \left(1 - \frac{z}{z_i} \right)$$

$$\sigma_w = 1.3 u_* \left(1 - \frac{z}{z_i} \right)$$

$$\frac{d\sigma_w}{dz} = -\frac{1.3 u_*}{z_i};$$

and the Lagrangian timescales

$$\tau_u = \tau_v = 0.07 \frac{z_i}{\sigma_v} \left(\frac{z}{z_i} \right)^{1/2}$$

$$\tau_w = 0.1 \frac{z_i}{\sigma_w} \left(\frac{z}{z_i} \right)^{0.8}.$$

4.4.2.2 Homogeneous profiles

For the case of homogeneous turbulence (i.e. constant within the boundary layer), the following mean boundary layer values are used:

$$\sigma_u = \sigma_v = u_*$$

$$\sigma_w = 0.65 u_*$$

$$\tau_u = \tau_v = 0.05\frac{z_i}{\sigma_u}$$

$$\tau_w = 0.05\frac{z_i}{\sigma_w}.$$

4.4.3 Unstable Conditions

Unstable or convective conditions occur where the air is buoyant due to heating from the surface. The boundary layer is deepened steadily by the action of thermals on the capping inversion, and reaches a maximum (which may be a km or two) by late afternoon. Turbulent mixing is due to both buoyant overturning and mechanical turbulence, which decay in the mixed layer after sunset. When the weather conditions are generally overcast and windy, and in some situations of transition, the heat flux to and from the surface is near zero, and the atmosphere is described as neutral.

4.4.3.1 Inhomogeneous turbulence

For skewed inhomogeneous turbulence the vertical velocity variance is determined from Hibberd and Sawford's (1994) profile adjusted to include a component for the mechanical generation of turbulence (by way of a sum of squares) using a mechanical term derived from the profiles in Brost et al (1982):

$$\sigma_w = \left[1.2w_*^2\left(1-0.9\frac{z}{z_i}\right)\left(\frac{z}{z_i}\right)^{\frac{2}{3}} + \left(1.8-1.4\frac{z}{z_i}\right)u_*^2\right]^{\frac{1}{2}}$$

so that

$$\frac{d\sigma_w}{dz} = \frac{1}{\sigma_w z_i}\left\{w_*^2\left(\frac{z}{z_i}\right)^{-\frac{1}{3}}\left(0.4-0.9\frac{z}{z_i}\right) - 0.7u_*^2\right\}$$

These formulae can also, of course, be applied in the neutral limit. A.R.Brown (private communication) has found from LES integrations that although formulae which exclude the mechanical contribution are inadequate, the inclusion of the full neutral component can give results which are a little excessive. A cube root sum of cubes may be preferable. The formulae will be reviewed when further experience has been gained. Similarly,

$$\sigma_u = \sigma_v = \left[0.4w_*^2 + (5-4z/z_i)u_*^2\right]^{\frac{1}{2}}$$

It will be noted these formulae give a profile for σ up to about $z/z_i = 1.3$. In addition, Sk=0.6 and C_0=1.0, this value was found to give better results than $C_0 = 2$ for the NAME 2 model.

The formula for the dissipation rate of TKE is a combination of convective and neutral terms from Luhar and Britter (1989) and a fit to the profile in Grant (1992), respectively:

$$\varepsilon = \left(1.5 - 1.2\left(\frac{z}{z_i}\right)^{\frac{1}{3}}\right)\frac{w_*^3}{z_i} + \frac{u_*^3(1-0.8z/z_i)}{kz}$$

subject to a minimum of 10^{-6}, and

$$\tau_{u,v,w} = 2\sigma^2_{u,v,w} / C_0\varepsilon$$

4.4.3.2 Homogeneous turbulence

For the simpler case of Gaussian homogeneous turbulence the profiles used are

$$\sigma_u = \sigma_v = \left[0.4w_*^2 + 3u_*^2\right]^{\frac{1}{2}}$$

$$\sigma_w = \left[0.4w_*^2 + 1.1u_*^2\right]^{\frac{1}{2}}$$

$$\varepsilon = 0.6w_*^3 / z_i + 1.2u_*^3 / kz_i$$

used to compute τ, as above; Sk=0.0, and C_0 = 1.0.

4.4.4 Free troposphere

Above the boundary layer fixed values are currently used:

$$\sigma_{u,v} = 0.5\text{ms}^{-1}$$

$$\tau_{u,v} = 300s$$

$$\sigma_w = 0.1\text{ms}^{-1}$$

$$\tau_w = 100\text{s}.$$

4.5 Boundary Conditions and Small-scale Entrainment

For each call to the advection routines particles are advected through a model timestep (typically 5, 10 or 15 minutes), either by a series of shorter variable timesteps (near-source scheme) or by a single step (long-range scheme).

4.5.1 Homogeneous Profiles.

When using homogeneous profiles particles can be maintained within the boundary layer during a model timestep by reflecting particles off the surface and boundary layer top. In unstable conditions where the skewed turbulence is applied then the

boundary condition used is one of skewed memory reflection, where w' is scaled by the absolute value of the ratio of the mean updraught velocity to the mean downdraught velocity when reflecting at the ground (w' becomes $-w'(1-p)/p$). The inverse of the probablility ratio is used in an analogous manner at the top of the mixed layer. Mixing across the boundary layer top therefore occurs only during what might be regarded as **large-scale entrainment:** through the movement of the boundary layer top from one model timestep to the next, or by particles in the boundary layer being advected to regions of differing boundary layer depths. In either case the turbulent components are reinitialised.

Alternatively the **small-scale entrainment** parametrization can be used at the boundary layer top (Thomson et al, 1996). This is a kinematic rather than a physically based theory: the physics resides in the determination of appropriate turbulence parameters. For a particle approaching the inversion from below, calculate

$$Arg^2 = \left\{ \frac{w'^2(old)}{\sigma_w^2(old)} + \log_e \frac{\sigma_w^2(new)}{\sigma_w^2(old)} \right\}.$$

If Arg^2 is negative, the particle is reflected at the inversion (modifying the velocity with the skew option, as described above). If it is positive, the particle is allowed to cross the interface with its velocity changing (at the interface, and for the remainder of the timestep) to

$$w'(new) = \sigma_w(new)\, Arg.$$

Particles approaching the inversion from the side with the smaller σ_w (essentially from above as the model is currently structured) are always transmitted, using the same expression.

4.5.2 Inhomogeneous Profiles.

When using inhomogeneous profiles particles are reflected from the surface as in the homogeneous case, but are not reflected at the boundary layer top, or reinitialised on passage through the inversion, as $\partial \sigma_w / \partial z$ is (at least piecewise) continuous, and the random walk includes a bias velocity as in equation (4.4). Turbulent components *are* reinitialised if particles cross the boundary layer top due to the boundary layer depth changing between timesteps ($\partial \sigma_w / \partial t$ is discontinuous) - in both homogeneous or inhomogeneous situations.

4.5.3 Long Range Scheme.

In the far field, the options are similar to those for the homogeneous near-source. Given the entrainment option, particles approaching the inversion from below are transmitted with a probability $\left(K(new)/K(old)\right)^{1/2}$, otherwise reflected. If a particle is transmitted the velocity is adjusted at the interface to

$$w'(new) = w'(old)\sqrt{K(new)/K(old)}.$$

As before, $K = \sigma_w^2 \tau_w$ is essentially greater below the inversion than above, so that particles approaching from above are always transmitted; the timestep must be constant.

4.6 Plume Rise.

A method of incorporating plume rise and inversion penetration has been developed based upon the work of G.A.Briggs (see Randerson 1984, Seinfeld 1986 and J.C.Weil in Venkatram and Wyngaard (eds) 1988). This was done in collaboration with F.B.Smith (Imperial College), and was designed to utilise the multiple particle structure of the model and the diffusion code. Plume rise is applied only with the inhomogeneous near-source diffusion option.

4.6.1 General Formulation.

The strategy adopted is to recognise that the wind at the stack top is not constant; when the fluctuating velocity is weak the plume temperature will be higher and the plume rise (for a short period) greater. The individual particles will have a random scatter about the middle of this fluctuating plume height. The plume height is

$$z_{pl}(t) = h(t) + h_s,$$

where h_s is the height of the stack and $h(t)$ the plume rise.

For particles released into an unstable boundary layer the fluctuating plume rise $h(t)$ is determined from

$$h(t) = \left\{ \frac{3 r_0^2 T_a R^2 X}{(0.4 + 1.2/R)^2 T_s} + \frac{3}{2} \frac{g(T_s - T_a) v_s r_0^2 X^2}{0.36 T_a U^3} \right\}^{1/3}, \quad (4.12)$$

where r_0 is the stack radius, v_s the emission velocity, the current wind strength

$$U = \left\{ (\bar{u} + u')^2 + (\bar{v} + v')^2 \right\}^{1/2},$$

X is the distance from source computed using $U\Delta t$, $R = v_s / U$, g is the gravitational acceleration and T_a, T_s the ambient air and emission temperatures respectively. U and T_a are defined for each particle at its time of release and remain constant for each individual particle for the duration of the plume rise, but different particles will have different values of U to give effect to the wind fluctuations. The two terms on the RHS represent momentum and (of much greater importance here) plume buoyancy.

4.6.2 Stable conditions

The stable formulation which follows is only appropriate if the plume particles are *released* in stable conditions, i.e. into a surface-based inversion or with the stack projecting above a capping inversion. Expression 4.12 is replaced with

$$h(t) = \varepsilon X^{\beta} / U^{\alpha}$$

where the parameters α,β and ε are taken from Table 4.1.

α	β	ε
1/3	0	$2.4(F/S)^{1/3}$
0	0	$5F^{1/4}S^{-3/8}$
1	2/3	$1.6F^{1/3}$

Table 4.1 Values of the parameters for the stable plume rise formulation.

F is a buoyancy flux parameter

$$F = gr_0^2 v_s [T_s - T_a] / T_s;$$

S is a stability parameter

$$S = g \frac{d\theta}{dz} / T_a$$

and θ is potential temperature. The minimum value of $h(t)$ computed from the three rows of the table is used. The two top rows do not need repeated calculation as they are not functions of X.

4.6.3 Turbulent fluctuations

To compute the displacement of particles scattered about the centreline of the instantaneous plume, it is assumed

$$z_p(t + \Delta t) = z_p(t) + \Delta h + h'(t) + w'(t)\Delta t$$

where z_p is the particle height, w' is the vertical component of the ambient mechanical turbulence, $\Delta h = h(t + \Delta t) - h(t)$, and the random increment due to buoyancy driven fluctuations, h', is generated from a Gaussian distribution with zero mean and standard deviation

$$\sigma_p = [W(t + \Delta t) - W(t)] / 4.3 = 0.14\Delta h .$$

That is, $h' = r\sigma_p$, where r is a random variable mean zero, standard deviation 1 and σ_p is derived under the assumption that the plume width $W(t) \approx 0.6h(t)$. A small timestep is necessary to prevent unrealistically large values of h', and negative Δh are not permitted. Allowance is made for reflection from the surface. The application of both the turbulent velocity components and fluctuations due to buoyancy to the particle displacements may seem excessive, as they are not additive in any simple way; however, preliminary tests suggested that a realistic spread is obtained. In a typical example in convective conditions the inclusion of w' increased the vertical spread σ_z

by about 10% over a plume-rise lifetime of a few minutes. It may be that w' is reduced or suppressed in the 'lofting' situation where a plume is levelling out beneath the capping inversion: this will require further testing against observations.

The mass flux from the chimney is from $F_m = \pi r_0^2 v_s$, and the plume potential temperature θ_p after a period t is estimated as

$$\theta_p(t) = \{F_m\theta_s + (F_m(t) - F_m)\theta_a\} / F_m(t),$$

where $F_m(t) = \pi W(t)^2 U / 4$, and θ_s, θ_a the emission and ambient potential temperatures.

Once z_p is obtained $\theta_p(t)$ is tested against the potential temperature θ_{zi} at the particle position. Then if $\theta_p(t) \leq \theta_{zi}$ the plume rise is terminated, the particle assumed passive, and the usual advection continued; otherwise the plume rise continues. The degree of penetration through the capping inversion clearly impacts upon the quantity of material left in the boundary layer, and available for subsequent mixing to the surface.

4.7 Implementation

The full random walk technique is applied to near-source particles, where an accurate description of plume growth is most important. At present the technique is applied to particles for a user-defined time period following release, chosen (e.g.) to represent the time required for particles to become well mixed through the boundary layer. A graduated application can be adopted: for a given particle inhomogeneous profiles are used for an initial period t_{in}, then homogeneous profiles for a subsequent period of t_h,. Finally, after a period of $t_{in} + t_h$, the long range scheme is applied, using homogeneous profiles. Note that any combination of profiles can be used by setting either or both of t_{in} and t_h to zero.

The skewed turbulence option in unstable conditions can be applied whether homogeneous or inhomogeneous profiles are used, for a user defined period of t_{sk} (subject to $t_{sk} \leq t_{in} + t_h$). In this way an optimum timestep can be used at the various stages of a simulation while still reproducing the essential features of dispersion.

Table 4.2 summarises the various options available in association with the diffusion parametrizations.

	Near-source Inhomogeneous	Near-source Homogeneous	Far-field
Small-scale entrainment	implicit	x	x
Skewed turbulence	x	x	
Plume rise	x		

Table 4.2 Diffusion schemes (x indicates option available)

4.8 Poles

For the global grid problems are possible near the polar regions. This arises because cell lengths in the east-west direction are very small. The *u* velocity component can cause a particle to 'spin' around the pole many times if it is very close to the pole. To prevent this the u component of both the velocity and the random perturbation due to diffusion is set to zero for particles close to the poles. The *v* velocity component is interpolated from the nearest two grid values.

With a latitude/longitude grid, as for the global version, the horizontal random walks can result in some slight poleward bias (D.J.Thomson, personal communication, has examined this situation). This could be a matter for concern in prolonged integrations, but it is considered that the NAME model is not significantly affected as for periods of a day or more as the spread of particles is primarily by the resolved winds, diffusion playing a relatively minor role (Maryon & Buckland, 1995).

4.9 Mixing by Convection

One potentially important mechanism for mixing particles in the vertical is deep convection, such as that associated with cumulonimbus. Material can be rapidly transported upwards throughout the depth of the atmosphere during deep convection, removing material from the boundary layer. Similarly, material can be brought down from upper layers by compensating downdraughts (generally weaker, but over larger areas). Whilst a detailed understanding of the role of deep convection in redistributing pollutant in the vertical is not available, a simple scheme (applied separately to the advection scheme) has been introduced to represent this enhanced vertical mixing.

Convective mixing is triggered only where convective cloud is present with a depth greater than η=0.3 (approx 300mb) and a base below η=0.8 (approx 800mb). All particles between the ground and cloud top are then considered to be in an updraught or downdraught, with the proportion of particles C_f (maximum 0.5) considered to be in an updraught being equal to aC_{mod}, where a is a coefficient less than unity (currently taken as 0.7) and C_{mod} the convective cloud fraction taken from unified model output. Each particle is then given a vertical velocity based on a simple vertical velocity profile i.e. for updraughts:

$$v_+ = r\left(\frac{\eta - \eta_{top}}{\eta_{base} - \eta_{top}}\right)v_c \qquad \eta<\eta_{base}$$

$$v_+ = rv_c \qquad \eta>\eta_{base}$$

and for downdraughts:

$$v_- = v_+\left(\frac{C_f}{1-C_f}\right);$$

where η is the particle height, η_{top} and η_{base} the cloud top and base respectively, v_c is the mean updraught convective velocity (currently assumed $1ms^{-1}$), and r is a random number chosen from a Gaussian distribution, mean=1 and unit variance. The downdraught is taken as applying only to particles in the free troposphere at present.

If the cloud fraction at the particle location is greater than or equal to the cloud fraction during the previous timestep then the probability of an updraught particle remaining in an updraught is

$$p = (1 - E\Delta t).$$

where E is an entrainment rate (currently set at $1.0 \times 10^{-4} s^{-1}$. This results in most updraught particles remaining in updraughts, with a small proportion lost to represent entrainment processes. To maintain a proportion C_f of particles in updraughts the probability of downdraught particles becoming updraught particles is then

$$p = \frac{C_f - (1 - E\Delta t)C_{f,old}}{1 - C_{f,old}}.$$

where $C_{f,old}$ is the cloud fraction during the previous timestep.

If the cloud fraction is smaller than the previous cloud fraction then fewer particles remain in updraughts, and the probability of an updraught particle remaining in an updraught becomes

$$p = (1 - E\Delta t)\frac{C_f}{C_{f,old}},$$

and the probability of a downdraught particle becoming an updraught particle

$$p = \frac{C_f - (1 - E\Delta t)C_f}{1 - C_{f,old}}.$$

Further work is planned to develop this scheme, for example by improving estimates of vertical velocities and entrainment rates.

5. LOSS PROCESSES

5.1 Introduction

The processes by which material is lost from the atmosphere include wet and dry deposition to the ground, radioactive decay and chemical reactions. Within the model these losses are applied on a particle basis, i.e. the mass of each particle is reduced each timestep, and for deposition processes the depleted mass added to surface deposition maps. Particles are never removed by deposition *in toto*, and lost to the integration. They can however be re-used if they drift clear of the domain in use or are depleted to a pre-defined, very low, mass (see Ryall & Kitchen, 1996).

5.2 Wet Deposition

For many pollutants wet deposition is the dominant means by which material is removed from the atmosphere to the ground. Two main processes are involved: washout, where material is 'swept out' by falling precipitation; and rainout (the most efficient), where material is absorbed directly into cloud droplets as they form by acting as cloud condensation nuclei. Rainout coefficients are dependent on the phase (i.e. water or ice/snow) and on the mechanisms for droplet growth, which differ for dynamic and convection clouds. Washout coefficients are also dependent on the precipitation type, for example snow flakes 'sweep' out a larger area than rain drops. Enhanced removal occurs where precipitation is orographically enhanced by the seeder/feeder mechanism.

The removal of material from the atmosphere by wet deposition processes is based on the depletion equation

$$\frac{dC}{dt} = -\Lambda C$$

where C is the air concentration, t is time, and Λ is the scavenging coefficient. The mass by which each particle is depleted can then be given by

$$\Delta m = m(1 - \exp(-\Lambda \Delta t)) \qquad (5.1)$$

where m is the mass of the particle at the start of the timestep. The scavenging coefficient Λ is usually defined by:

$$\Lambda = A r^B \qquad (5.2)$$

where r is the rainfall rate and A and B are coefficients defined for different types of precipitation (e.g. dynamic, convective, rain and snow), and different deposition processes (e.g. rainout, washout and orographically enhanced precipitation).

5.2.1 Scavenging Coefficients

Table 5.1 summarises the scavenging coefficients currently implemented within the model and when they are applied. The coefficients, based on observational data and detailed cloud modelling, have been supplied by Dr T Choularton at UMIST, who has collaborated with the NAME team over a long period.

Note that orographically enhanced rainfall coefficients are used only where (i) the precipitation data originate from FRONTIERS processed data (i.e. only over the UK); (ii) orographic enhancement has been applied to the FRONTIERS data; and (iii) the relief is greater than 150 m.

	Λ(s^{-1}) Rain (Below Freezing Level)		Λ(s^{-1}) Snow (Above Freezing Level)		When Applied
	Convective	Dynamic	Convective	Dynamic	
Washout	$8.4 \times 10^{-5} r^{0.79}$		$8.0 \times 10^{-5} r^{0.305}$		-Below Cloud base
Rainout	$3.36 \times 10^{-4} r^{0.79}$	$8.4 \times 10^{-5} r^{0.79}$	$3.36 \times 10^{-4} r^{0.79}$	$8.0 \times 10^{-5} r^{0.305}$	-Between cloud base and cloud top
(Seeder/ Feeder)	$3.36 \times 10^{-4} r^{0.79}$ +		$1.0 \times 10^{-3} r^{0.79}$		-Below 1200 m, -Topography>150m -FRONTIERS Orographic flag

Table 5.1 Scavenging coefficients used in the name model, r is rainfall rate (mm/hr)

5.2.2 Meteorological data

Precipitation

Precipitation rates and cloud data are taken from the nearest model grid value and interpolated in time; whilst all other met data are linearly interpolated in space to particle positions, and in time to the start of the current model time step.

Dynamic cloud information is unavailable from the Unified Model, so fixed pressure levels of 900 hPa and 700 hPa are currently used for the dynamic cloud base and top

As the high resolution precipitation fields do not distinguish between convective and dynamic precipitation, the model ratio of convective to dynamic precipitation is used to apportion the precipitation when high resolution rainfall data are used.

The temperature at the particle position is used to determine whether the particle is above or below the freezing level (0°C).

5.2.3 Implementation

Appropriate values for the coefficients A and B (equation 5.2) are determined separately for convective and dynamic precipitation, depending on the particle height relative to the appropriate cloud base, cloud top and freezing level. The coefficients for snow/ice are used above the freezing level, and coefficients for rain below the freezing level. The convective precipitation rate will generally underestimate the true convective precipitation rate, as it represents the mean rate over the whole grid cell, even though the precipitation may only be occurring over a fraction of the area. The convective precipitation rates r_{con} are therefore obtained from

$$r_{con} = r / C_f ,$$

where C_f is the convective cloud amount fraction. The particle mass is then depleted for each species according to Equation 5.1 for both the convective and dynamic precipitation components. For convective precipitation the depletion is applied to the fraction C_f of the particle mass---this does not simply compensate for the above enhancement of the precipitation rate, as the scavenging formulae are non-linear.

The total depleted mass for each species is integrated for each of the wet deposition fields, and expressed as a deposition per unit area.

5.3 Dry Deposition

Whilst wet deposition is the dominant loss process for most pollutants, dry deposition is still an important loss process. The basis of the parametrization is that the flux F of pollutant to the ground is proportional to the concentration C of the pollutant above the ground:

$$F = \upsilon_d C$$

where the constant of proportionality υ_d is known as the deposition velocity. Both υ_d and C are defined at a reference height z, typically 1-2m. Assuming that concentrations are constant over a layer of depth z_s, adjacent to the surface, then

$$\frac{dC}{dt} \approx -\frac{F}{z_s} = -\frac{\upsilon_d}{z_s} C$$

where t is time. The mass loss for a particle within the layer z_s can then be written as

$$\Delta m = -\frac{\upsilon_d}{z_s} m \Delta t .$$

Currently z_s is taken as the boundary layer depth.

5.3.1 Deposition Velocity υ_d

A resistance analogy parametrization is used to determine the deposition velocity at each particle position:

$$\upsilon_d = \frac{1}{R_a + R_b + R_c}$$

where R_a is the aerodynamic resistance, R_b is the laminar layer resistance, and R_c is the surface resistance.

Aerodynamic Resistance

The aerodynamic resistance is used to specify the efficiency with which material is transported to the ground by turbulence, and is independent of the pollutant type. A commonly used expression adopted for application here is

$$R_a = \frac{1}{ku_*}\left[\ln\left(\frac{z+z_0}{z_0}\right) - \Psi_h\left(\frac{z+z_0}{L}\right)\right]$$

where k is von Karmans constant (0.4), u_* is surface stress, z_0 is the roughness length and L is the Monin-Obukhov length. Ψ_h is a stability correction function for temperature, defined here in unstable conditions by

$$\Psi_h = 2\ln\left[\frac{\left(1+\phi_m^2\right)}{2}\right]$$

where

$$\phi_m = \left(1 - 16\frac{z+z_0}{L}\right)^{1/4};$$

in stable conditions by

$$\Psi_h = -5\left(\frac{z+z_0}{L}\right).$$

In the limits as $|L|$ becomes large Ψ_h tends to zero, and the conditions approximate neutral.

Laminar Resistance

The laminar resistance represents the resistance to transport across the thin quasi-laminar layer adjacent to the surface. For gaseous pollutants, and the range of particulates $0.1 - 10\mu$ m (of particular relevance to releases of a number of radioactive species such as caesium), we take

$$R_b = \frac{2}{0.72ku_*}\left(\frac{\nu}{D_i}\right)^{2/3}$$

where ν is the kinematic viscosity of air ($0.15\text{cm}^2\text{s}^{-1}$) and D_i is the molecular diffusivity of pollutant. For practical purposes it is reasonable to approximate R_b to a fixed value: i.e.

$$R_b = \frac{8}{u_*}.$$

Surface Resistance

The surface resistance characterises the resistance to capture by the surface itself. It is often the most important of the resistances, yet it represents a complex process and remains the least well understood. It depends both on the pollutant and on the nature of the surface (e.g. crops, forest, concrete etc.), which may itself be dependent on

other factors (e.g. season, time of day, atmospheric conditions etc., see Erisman 1994a,b,c, Baldocchi et al 1987 & Baer & Nester 1992).

Given the uncertainties in determining surface resistance and the wide range of values found in the literature (e.g. Walcek et al 1986, Sehmel 1980), a fixed value of R_c is used for each species. In general, the more reactive a species the lower its surface resistance.

6.3.2 Gas to particulate conversion.

After emission, iodine-131 gas is steadily taken up by particulate aerosol, with a corresponding alteration to the deposition velocity. Starting with equations for the time rate of change of gaseous and particulate concentration it is possible to derive an expression for the net loss of iodine-131.

$$\frac{dC}{dt} = -\left(\frac{v_d}{z_s} + \frac{1}{\tau}\right)C(t) + \frac{C_g(0)}{\tau}\exp\left(-\frac{w_d}{z_s}t\right)$$

where $C_g(0)$ is the initial concentration of the gas and v_d, w_d are the gaseous and particulate deposition velocities, respectively. The conversion timescale τ has been estimated at 47 days from the emissions from Chernobyl reaching Britain.

5.4 Turbulent Deposition

Turbulent (or occult) deposition occurs where 'polluted' cloud droplets directly impact to the ground. This generally occurs when moist low level air is saturated to form hill capping cloud as it is advected and lifted over higher ground. Whilst strictly a wet deposition process occult deposition is parametrized in terms of a dry deposition velocity. The dry deposition velocity used is related to the value for momentum (as determined in field observations by T. Choularton's team at UMIST) i.e.:

$$v_d = \frac{0.8}{R_a}$$

Turbulent deposition is only applied where the liquid water content is greater than 10^{-4} kg/kg, the friction velocity u_* is greater than 0.2 m/s (to avoid applying occult deposition in regions with still-air radiation fog), and where the relief exceeds 150 m.

5.5 Radioactive Decay

For radioactive materials mass is lost by radioactive decay. The governing equation is

$$\frac{dm}{dt} = -\frac{m}{aq}$$

where q is the half-life, a is a constant (=1.4427). The mass of a particle can then be written as

$$m_2 = m_1\left(1 - \frac{\Delta t}{aq}\right).$$

5.6 Chemistry

For sulphur modelling sulphur dioxide is converted to sulphate by the simple linear reaction:

$$SO_2(S) = SO_2(S)(1 - kt\Delta t)$$

$$SO_4(S) = SO_4(S) + SO_2(S)kt\Delta t \quad .$$

Where kt is a transformation coefficient, currently fixed at $2.8 \times 10^{-6}\ s^{-1}$.

6. AUTOMATIC ADJUSTMENTS TO MODEL PRODUCTS

As a consequence of model error, forecast error and the natural randomness and variability of the atmosphere the model meteorology will always differ from reality to some extent. NAME 2 has several facilities for modifying the model products, and assumptions of source strength, by comparing the model output with the observations of radioactivity which would be made widely in the event of a serious nuclear accident. One facility (manual rather than automatic) is to 'bend' the near-source plume by biasing the random walk, if the real plume is observed to set off at an angle to the simulated one. There are also automated facilities for adjusting the plume spread by means of an artificial 'diffusivity' and for estimating the strength of a source from measured concentration data. Given a reasonable coverage of observed air concentration fields at a given time, the 'actual' and modelled fields can be used with a least squares technique to estimate the source strength, as a function of both time and height. Thus there are two main stages: (i) plume spread adjustments and (ii) source reconstitution; these are discussed in sections 6.1 and 6.2. A full description of the technique can be found in Maryon and Best (1995). These techniques can be applied only with K-type diffusion schemes(i.e. the far-field scheme), with fixed timesteps.

6.1 Plume spread

The model inaccuracies are likely to be particularly serious where the winds are strong, and rapidly changing, as near an active, travelling depression. The area over which the model predicted plume overlaps with the observed field is likely to be insufficient in these circumstances. To improve the overlap the model is re-run iteratively, adjusting the diffusion coefficient (up or down) to obtain an overlap between the observed and model air concentration fields between 95 and 100%. The downward adjustment may be required to prevent unrealistically wide spreads of model particles before a near 100% coverage is obtained. The change in diffusion coefficient is related to the time rate of change of wind velocity, as errors are likely to be related to the magnitude of the wind shift: i.e. a modified diffusion coefficient K' used for each particle is calculated from

$$K' = (\beta|\varepsilon| + K^{1/2})^2$$

where β is an arbitrary user-defined coefficient, ε is the wind change at the particle location, and K is the diffusion coefficient. As K is defined in terms of the velocity variance σ and Lagrangian timescale τ this becomes

$$\sigma'^2\tau = \left(\beta|\varepsilon| + \sqrt{\sigma^2\tau}\right)^2.$$

where σ'^2 is a modified velocity variance. The value of β is changed using an iterative scheme until a suitable overlap is found.

6.2 Source reconstitution

The source emission profile is broken down into M 'slots', each describing a time window and vertical slab for which an estimated emission is required. Two vertical slabs are probably the most that can be realistically adopted. Let the model emissions for each slot be $e_i'(0)$, i=1,2..M and the corresponding 'real' emissions $e_i(0)$, i=1,2..M; then at a given time t in a particular grid cell, j,

$$\sum_{i=1}^{M} a_{ij} e_i(0) = A_j$$

where A_j is the measured activity/mass in the grid-cell j, and a_{ij} are coefficients representing the proportion of each $e_i(0)$ contributing to A_j. Then if there are N grid cells with observed mass, and $N > M$, a least squares solution for $e_i(0)$ can be found (Maryon and Best (1995). Introducing a weighting, ω_j, to represent the confidence in the model simulation for grid cell j, we minimise

$$\sum_{j=1}^{N} \omega_j \left[A_j - \sum_{i=1}^{M} a_{ij} e_i(0) \right]^2$$

yielding the 'normal equations'

$$\frac{d}{d[e_p(0)]} \left[\sum_{j=1}^{N} \omega_j \left(A_j - \sum_{i=1}^{M} a_{ij} e_i(0) \right)^2 \right] = 0 \quad p = 1,2\ldots, M.$$

From this the linear system

$$\sum_{i=1}^{M} e_i(0) \sum_{j=1}^{N} \omega_j a_{pj} a_{ij} = \sum_{j=1}^{N} \omega_j a_{pj} A_j \qquad (6.1)$$

is derived, which can be solved for the $e_i(0)$ using matrix operations.

The weighting factors ω_j are currently based on the average ratio of final to initial particle mass for all particles within the grid cell; thus grid cells in which particles

have lost a significant fraction of their mass due to depletion processes (and are therefore less reliable) contribute less to the solution. Later the reliability of observations may be incorporated in the weighting. Processing of radiological data to produce fields conformable with the structure of NAME 2 is by a software package supplied by AEA Technology Consulting Services, though at the time of writing this is yet to be brought into full operational use.

6.3 Implementation

Given that an observed air concentration field is available at time t_1 resulting from a release at time t_0, a standard model simulation is performed from time t_0 to t_1 with release slots defined to correspond with each of the slots required for the emission reconstitution. A best guess of the emission rate, or default value, is used for each slot. At the end of the run the emission from each slot is calculated from equation 7.1, together with the overlap between the observed and model predicted air concentration fields. If the overlap is too small the value of β is incremented iteratively by a user-defined amount until it exceeds 95% . If it exceeds 99% β is decreased using a smaller decrement. Thus a coverage between 95 and 99% is obtained (anything larger is bound to be associated with excessive spread of the modelled plume). The number of iterations is confined to a user-defined maximum. At present this procedure can only be carried out for one time, t_1, during a model integration, so that repeated runs would be necessary to deal with subsequent observational fields.

7. OUTPUT

7.1 Fields

Fields of diagnosed data, such as air concentrations and depositions, can be calculated and output on any of the unified model grids, irrespective of the resolution of the input data used to advect and deplete particles. In addition, fields can be output on (i) a 20 km resolution grid covering the UK based on the national grid; (ii) a user-defined latitude/longitude grid; and (iii) the high resolution rainfall grid. As well as diagnosed fields, meteorological fields used in the model can be output. Fields are output at user-defined intervals (the minimum interval is the model timestep), based on either UTC times or on time since the start of release.

7.2 Time series

Detailed time series of diagnosed values or of the meteorological data used by the model can be generated at an arbitrary number of user-defined locations, with values for each model timestep (meteorological data are linearly interpolated from adjacent data times).

7.3 Profiles

In addition to fields and timeseries it is possible to generate vertical profiles of air concentrations or of meteorological data used by the model. These are output at the

same time intervals as the fields, for each of the locations for which time series data are requested.

7.4 Graphics

For APR purposes data are copied to a UNIX workstation for graphical display. A windows type interface has been written using the PV-WAVE data visualisation package to readily select and display model output.

Some Examples of NAME output are shown in Figures 5 to 10. Figure 5 shows the particle positions 96 hours after the start of a continuous release from 53.80N 001.55W at a rate of 1g/s. Figures 6 and 7 show the resultant air concentration and total deposition fields analysed on the regional grid. Figure 8 shows a time series trace of air concentration and Figure 9 a vertical profile of air concentration. Figure 10 shows a particle plot from the sulphur model; note the individual plumes from power stations.

8. DOE TRANSMISSION SOFTWARE

In the event of an actual emergency NAME model output can be transmitted onto the RIMNET system. where it can be displayed in the Governments Department of Environment Office which would become the Technical Coordination Centre controlling the national response to a nuclear emergency. The software is provided and supported by Hunting's Engineering Ltd.

Diagnostic fields (boundary layer air concentrations, dosages, wet, dry and total depositions) are provided on a subsection of the global grid (covering UK and environs) and on the mesoscale custom grid (see Maryon and Ryall, 1996). Wet and total depositions can also be transmitted on the ERR grid. Weekly tests are performed to ensure correct operation of the system

9. PLANNED MODEL IMPROVEMENTS

There are many areas in which the model could be improved and developed; this section briefly discusses the main topics that it is hoped will be addressed in the near future.

9.1 Meteorological data

(i) At present meteorological data are used from only a subset of the available NWP vertical levels. As increased computing memory and speed becomes available further vertical levels will be added for increased vertical resolution, especially on the regional and global grids.

(ii) Improvements to the high resolution rainfall package, perhaps by replacement or addition with NIMROD fields.

9.2 Physical Processes

(i) The diffusion scheme above the boundary layer (i.e. the free troposphere) is relatively simple, using fixed turbulent properties. This needs to be improved to identify the effects of strong wind shear, turbulence due to breaking gravity waves etc.

(ii) Improved parametrisation of vertical mixing by deep convection is required, with better estimates of vertical fluxes as a function of height and cloud details.

(iii) Improved estimates of dynamic cloud base and thickness are required for wet deposition.

(iv) Further work on the surface resistance parametrisation is required for more accurate dry depositions.

9.3 Further Applications

(i) Under contract from HMIP the sulphur model will be assessed for forecasting sulphur air concentrations and depositions over the UK, through comparisons with observational data. An attribution package will also be developed, for determining the relative contribution of various sources to a given receptor.

(ii) The model will be used to investigate the long range transport of CFC's. Comparisons with observed levels at Mace Head (Western Ireland) will help assess the advection schemes, as CFC's are not subject to any short-term deposition or loss processes.

(iii) An ozone model will be developed by incorporating a chemistry package (54 species including NOx, SOx, & VOC's) .

10. REFERENCES

Baer M & Nester K (1992) 'Parametrisation of trace gas dry deposition velocities for a regional mesoscale diffusion model' *Ann. Geophysicae*, **10**, 912-923

Baldocchi D D, Hicks B B & Camara P (1987) 'A canopy stomatal resistance model for gaseous deposition to vegetated surface' *Atmos. Environ.*, **21**, 91-101

Brost R A, Wyngaard J C & Lenschow D H (1982) 'Marine stratocumulus layers> Part II: Turbulence budgets' *J. Atmos. Sc.* **39**, 818-836.

Erisman J W (1994) 'Evaluation of a surface resistance parametrisation of sulphur dioxide' *Atmospheric Environment*, **28**, 2583-2594

Erisman J W & Baldocchi D (1994) 'Modelling dry deposition of SO_2' *Tellus*, 46B, 159-171

Erisman J W, Pul A V & Wyers P (1994) 'Parametrisation of surface resistance for the quantification of atmospheric deposition of acidifying pollutants and ozone' *Atmos. Environ.*, **28**, 2595-2607

Grant A L M (1992) 'The structure of turbulence in the near-neutral atmospheric boundary layer' *J. Atmos. Sc.* **49**, 226-239.

Hanna, S.R. (1982) 'Applications in air pollution modelling. In: Atmospheric Turbulence and Air Pollution Modelling' Ed.F.T.M. Nieuwstadt and H. van Dop, D Reidel Publishing Company, Dordrecht, Holland.

Hibberd, M.F. and Sawford, B.L. (1994) 'A saline laboratory model of the planetary convective boundary layer' *Boundary-Layer Met.*, **69**, 229-250.

Hudson, B. and Thomson, D.J. (1994) 'Dispersion in convective and neutral boundary layers using a random walk model' Met O (APR) Turbulence and Diffusion Note No. 210.

Hurley, P.J. and Physick, W.L.(1993) 'A skewed homogeneous Lagrangian particle model for convective conditions' *Atmospheric Environment*, **27A, No. 4**, 619-624.

Kitchen K P (1993) 'Nuclear Accident Response Model Program Documentation, Version 2' MetO(APR) Internal Technical Memorandum No.21

Luhar, A.K. and Britter, R.E (1989) 'A random walk model for dispersion in inhomogeneous turbulence in a convective boundary layer' *Atmospheric Environment*, **23**, 1911-1924.

Maryon R H (1993) 'Supplementary Notes on the Structure and Parametrization of NAME' MetO(APR) Internal Technical Memorandum No.21, Version 2.

Maryon R H & Best,M.J. (1992) 'NAME, ATMES and the boundary layer problem' Internal Met Office report: Met O(APR) TDN No. 204

Maryon,R.H. & Best,M.J. (1995) 'Estimating the emissions from a nuclear accident using observations of radioactivity with dispersion model products. *Atmospheric Environment*, **29**, 1853-1869.

Maryon, R.H. and Buckland, A.T. (1994) 'Diffusion in a Lagrangian multiple particle model: a sensitivity study' *Atmos. Environ.*, **28**, 2019-2038.

Maryon R H & Buckland A T (1995) 'Tropospheric dispersion: the first ten days after a puff release'. *Q.J.R. Meteorol. Soc.* **121**, 1799-1833.

Maryon R H & Ryall D B (1996) 'NAME 2: A users' guide to the UK Nuclear Accident Response Model' Met O(APR) Internal Technical Memorandum No. 28 Version 2.

Maryon R H, Smith F B, Conway B J & Goddard D M (1991) 'The UK Nuclear Accident Model', *Progress in Nuclear Energy*, **26, No. 2**, 85-104.

Physick, W L. and Maryon, R.H. (1995) 'Near-source turbulence parametrization in the NAME model' Met O(APR) TDN No. 218.

Randerson, D (Ed.) (1984) 'Atmospheric science and power production', Washington, US Department of Energy, Office of Energy Research.

Ryall D B & Kitchen K P (1996) 'NAME 2: Model Documentation' Met O(APR) Internal Technical Memorandum No. 27

Sehmel, G.A. (1980) 'Particle and dry deposition: a review' *Atmos. Environ*, **14**, 983-1011

Seinfeld, J.H. (1986) 'Atmospheric chemistry and physics of air pollution', New York, John Wiley and Sons.

Thomson, D.J. (1987) 'Criteria for the selection of stochastic models of particle trajectories in turbulent flows' *J. Fluid Mech.*, **180**, 529-556.

Thomson, D J, Physick, W L and Maryon, R H (1996) 'Treatment of interfaces in random walk dispersion models', in preparation.

Venkatram, A and Wyngaard, J.C. (Eds.) (1988) Lectures on Air Pollution Modeling, American Meteorological Society, Boston.

Walcek C J, Brost RA & Chang J S (1986) 'SO_2, sulphate and HNO_3 deposition Velocities computed using regional landuse and meteorological data' *Atmos. Environ.*, **20**, 949-964.

Wilson, J.D., Legg, B.J. and Thomson, D.J. (1983) 'Calculation of particle trajectories in the presence of a gradient in turbulent-velocity variance' *Boundary-Layer Met.*, **27**, 163-169.

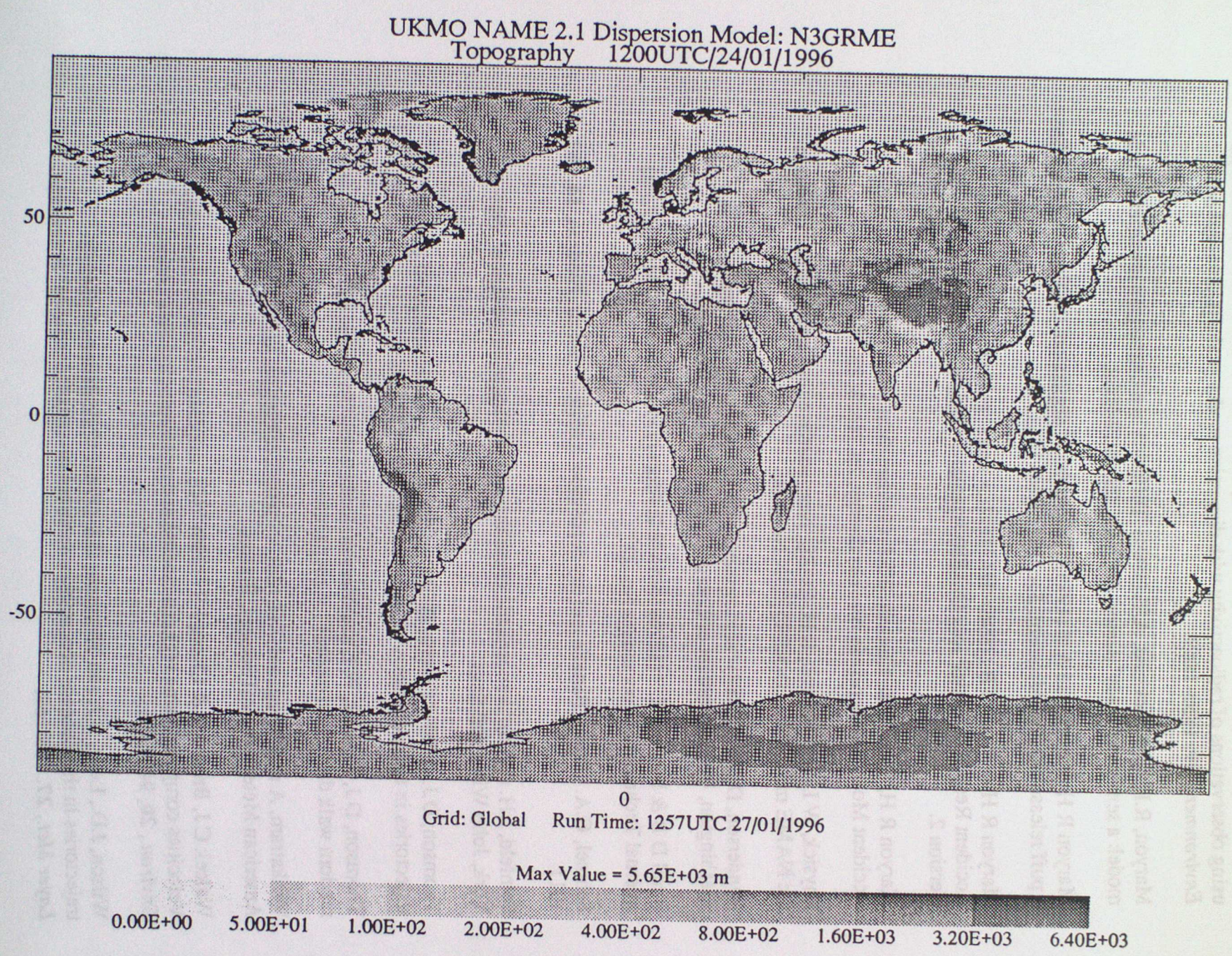

Figure 1 Global grid and topography

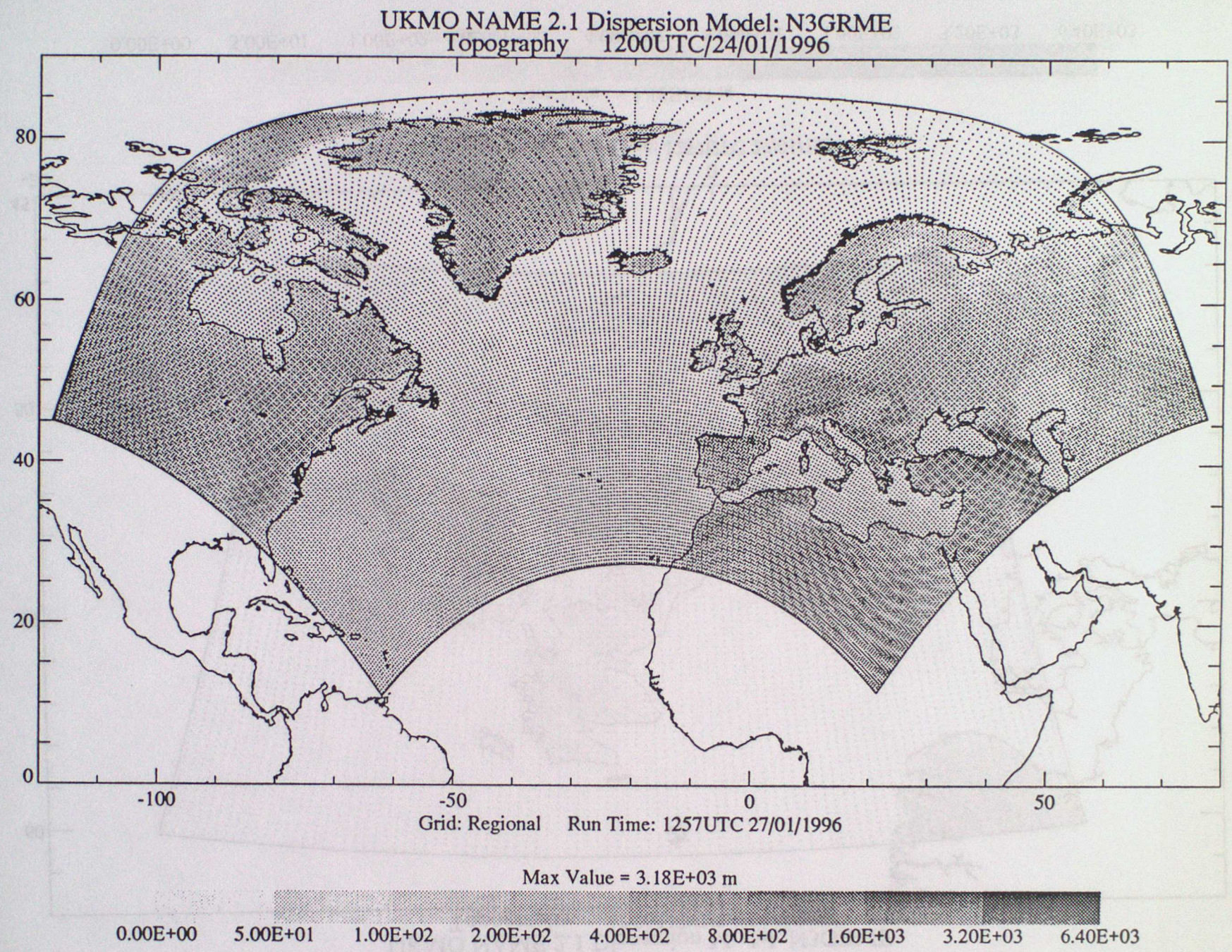

Figure 2 Regional (limited area) grid and topography

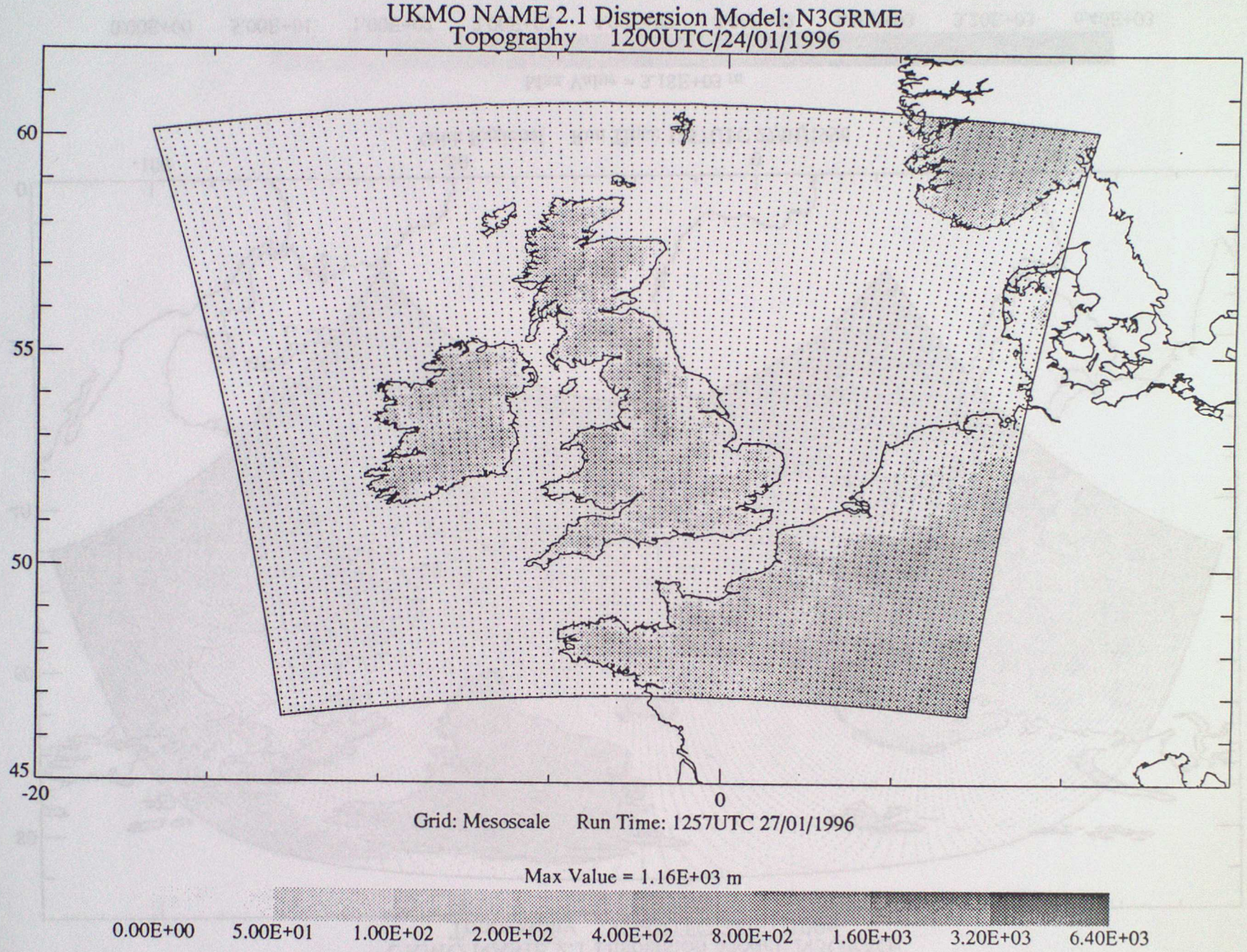

Figure 3 Mesoscale grid and topography

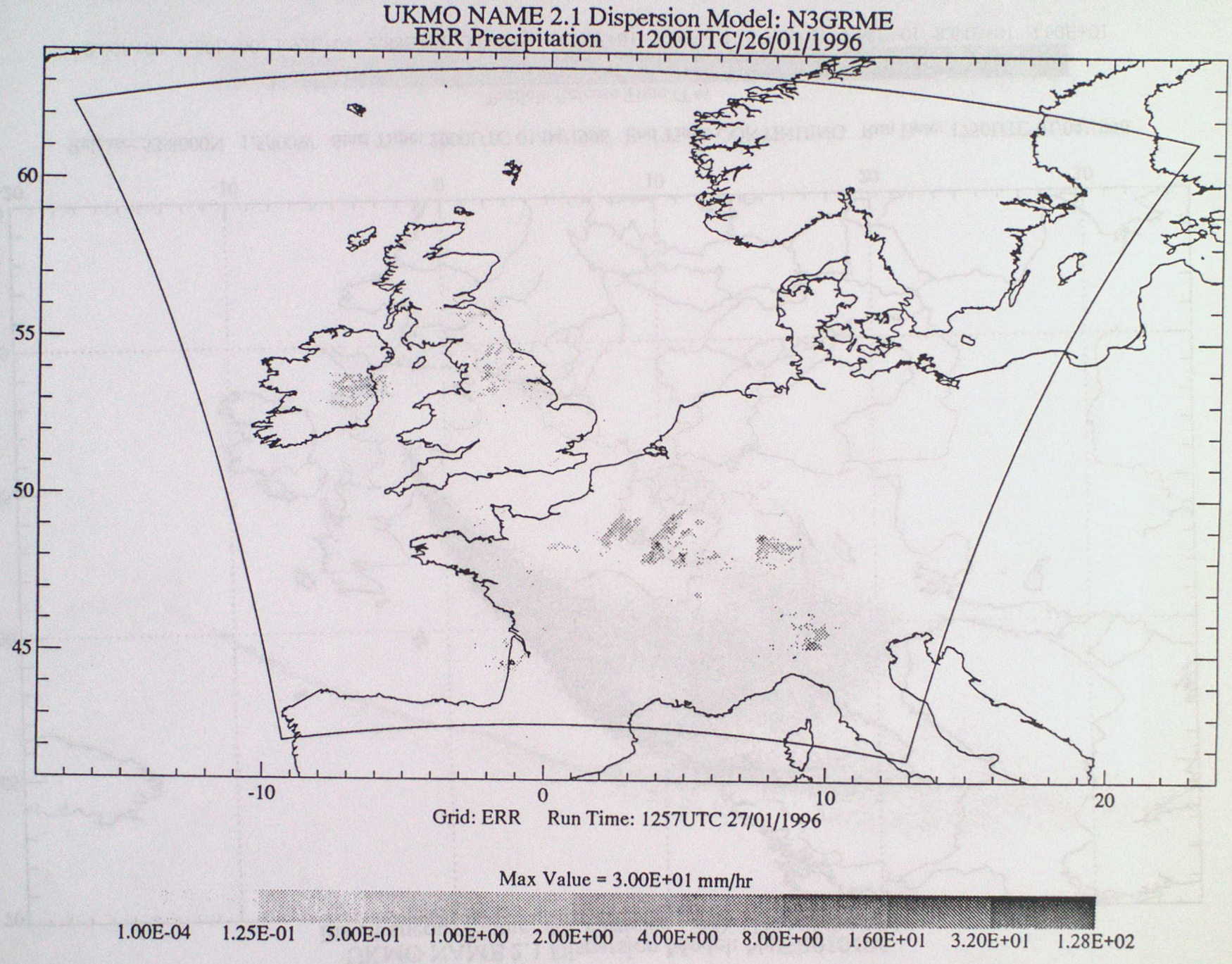

Figure 4 Example high resolution precipitation field and grid limits

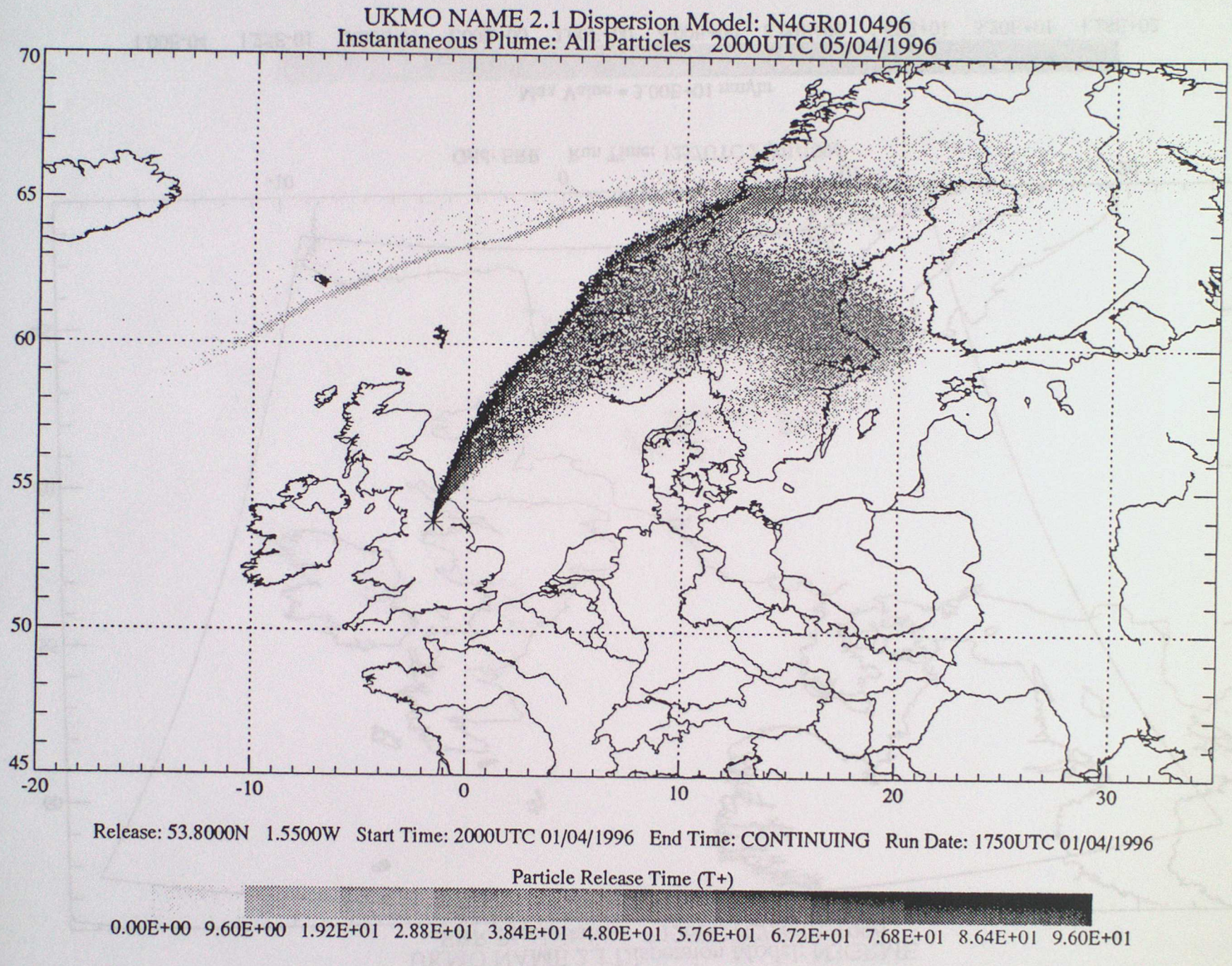

Figure 5 Particle plot at T+96 (older particles shaded lighter)

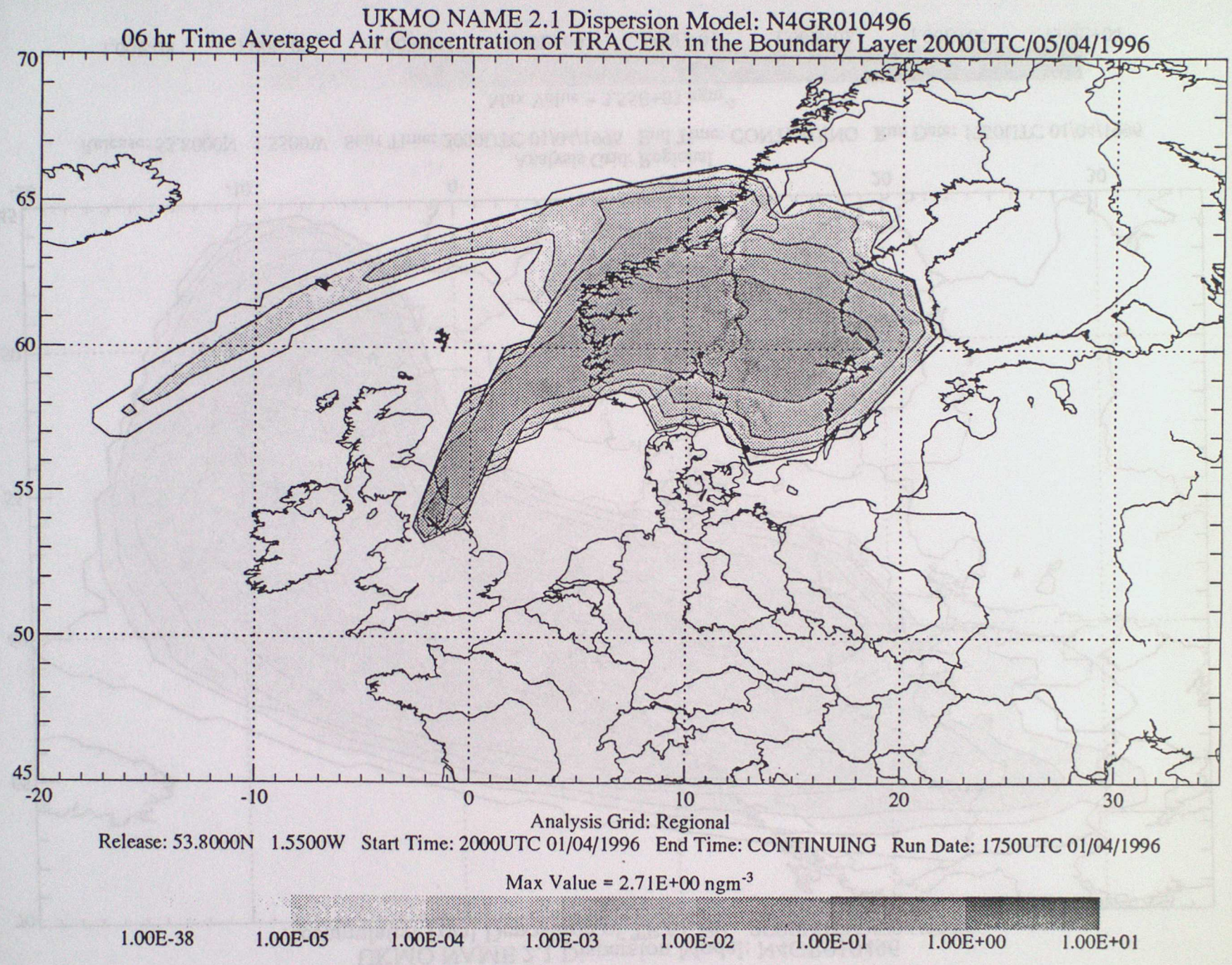

Figure 6 Air concentration at T+96

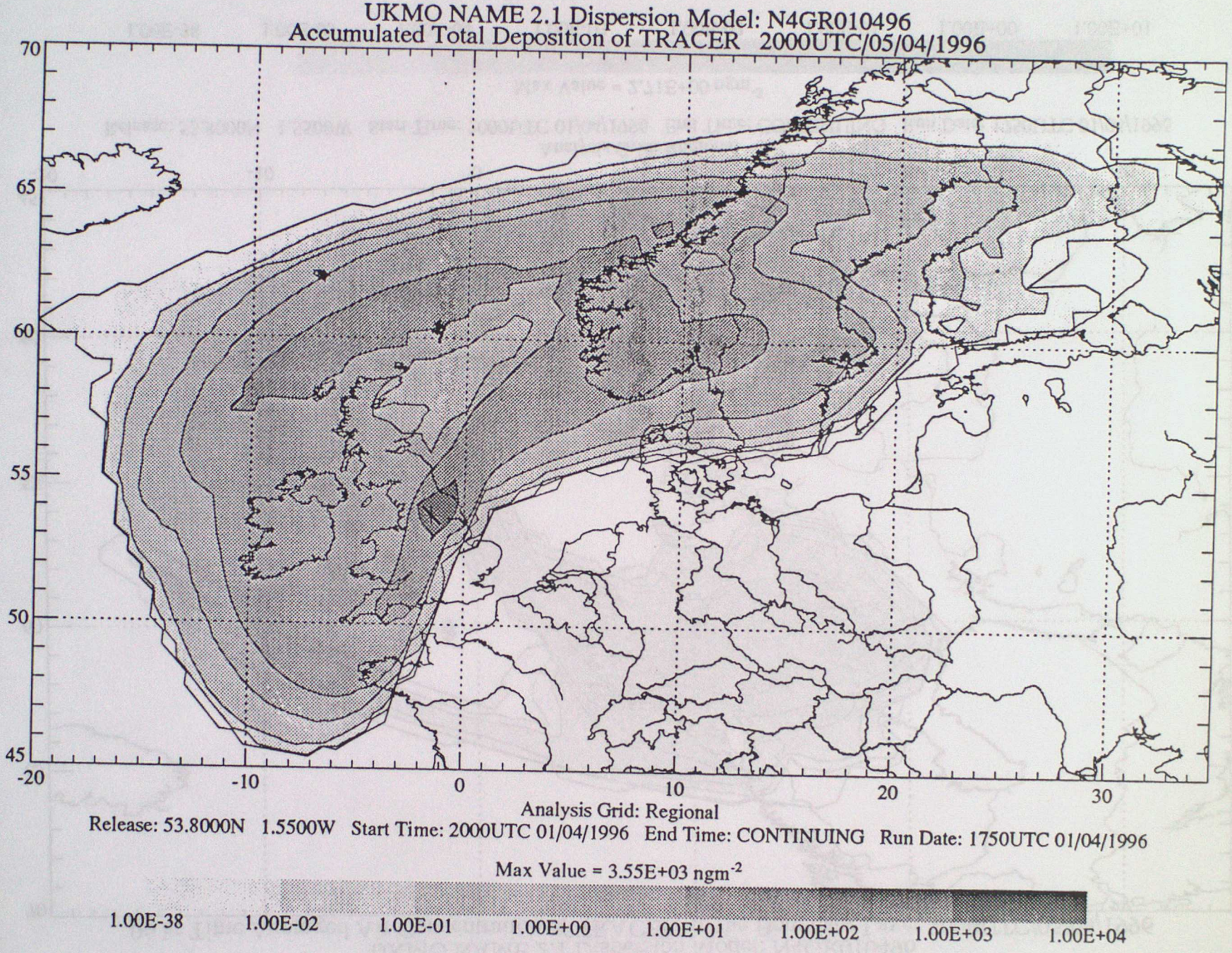

Figure 7 Total accumulated deposition at T+96

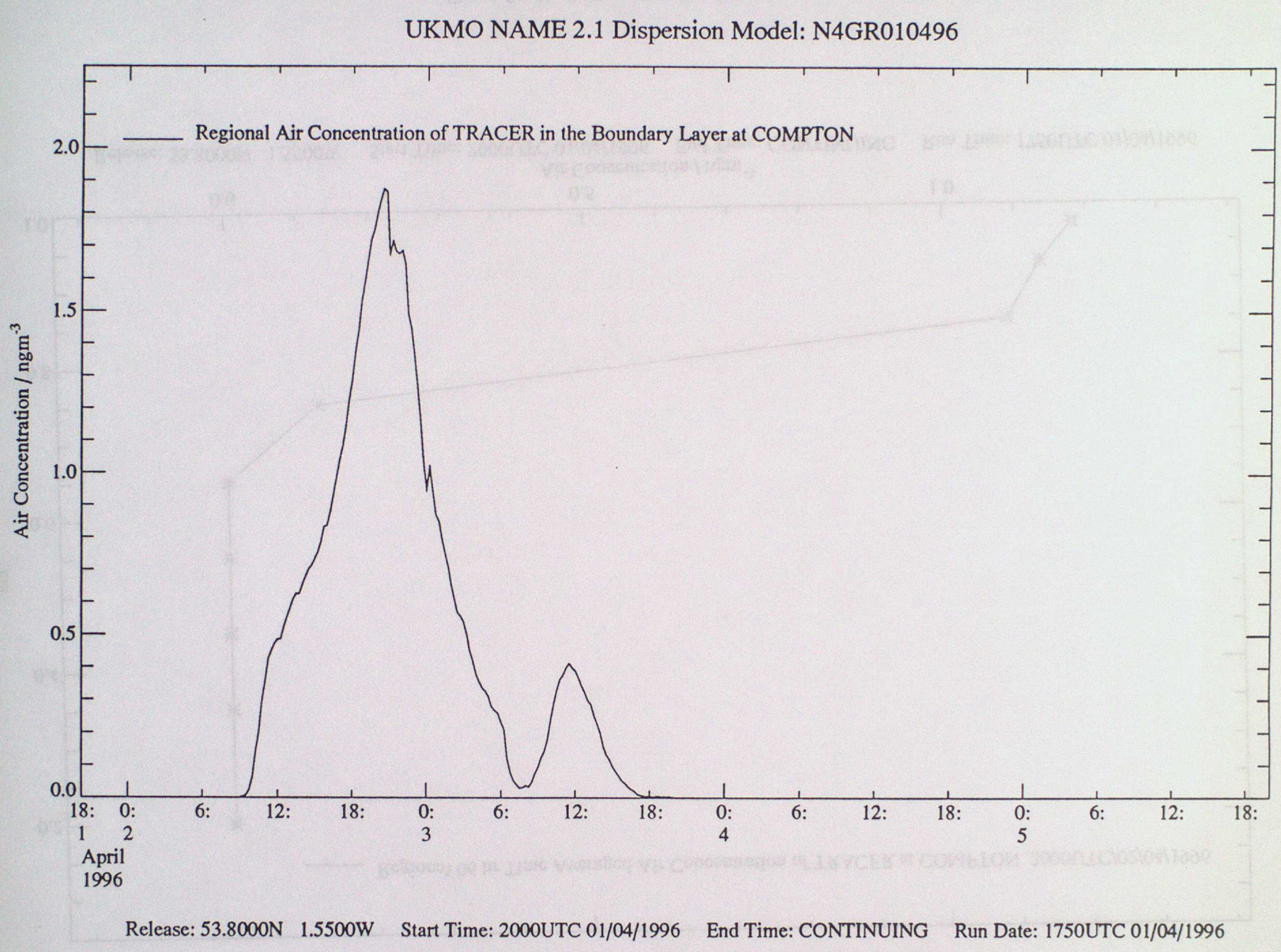

Figure 8 Time series of air concentration at Compton (50.9671N 002.1537W)

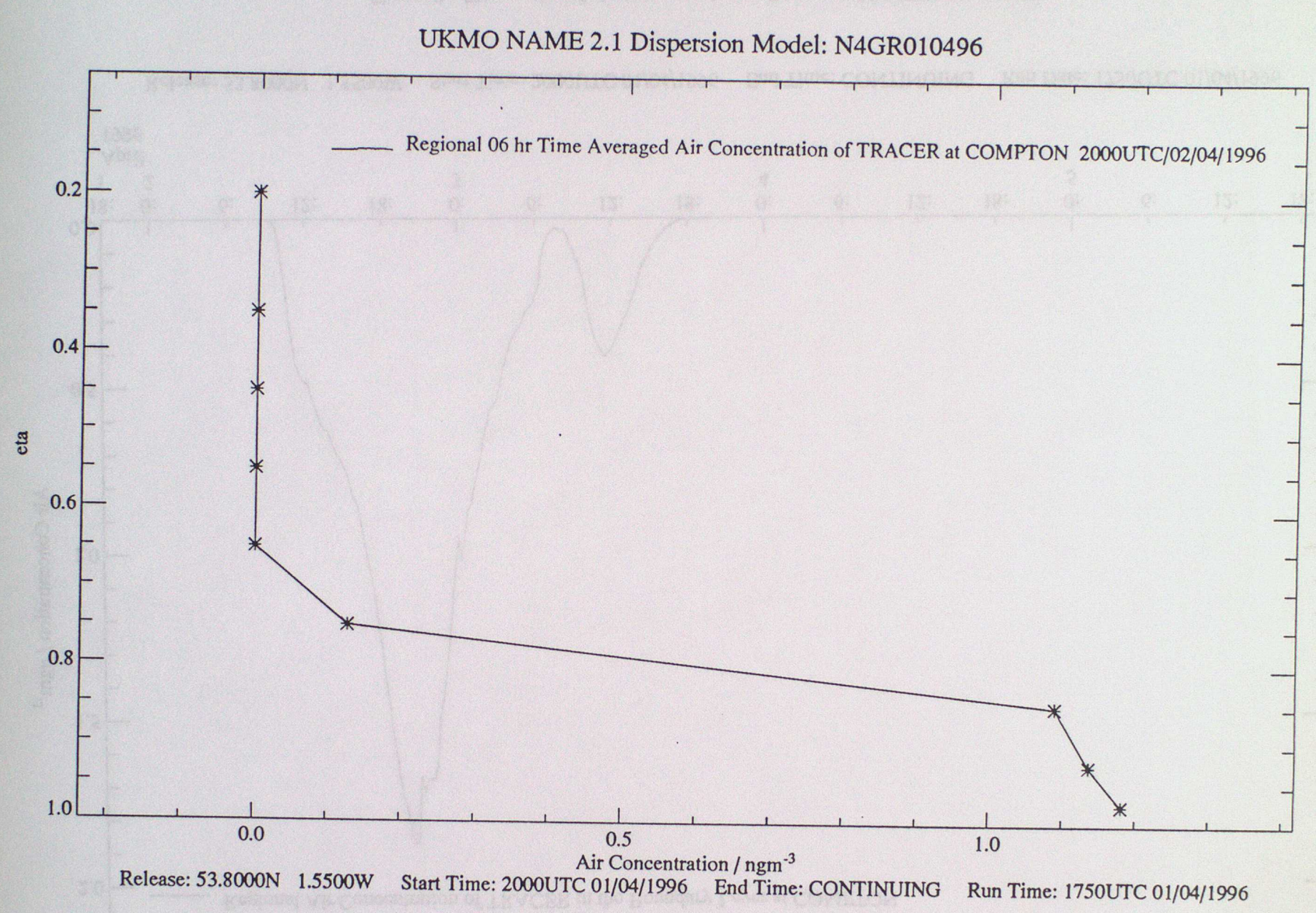

Figure 9 Vertical profile of air concentration